DIRECT MEASUREMENT OF DISSIPATION IN PHONONIC CRYSTAL AND STRAIGHT TETHERS FOR MEMS RESONATORS

Vikrant J. Gokhale[1,2] and Jason J. Gorman[1]
[1] National Institute of Standards and Technology, Gaithersburg, MD, USA
[2] Electrical Engineering and Computer Science, University of Michigan, Ann Arbor, MI, USA

ABSTRACT

This paper presents optical measurements of the dynamic strain profiles along the tethers of microelectromechanical resonators and relates them to mechanical quality factor (*Q*). Such measurements allow for the quantification of tether dissipation and fair comparison between various tether designs. Our experiments present the first systematic comparison between the best-performing conventional tethers with one-dimensional phononic crystal (PnC) tethers for silicon bulk acoustic resonators, and demonstrate more than 3× improvement in *Q* when the PnC tethers are used. The spatial decay rate of the mechanical strain profile along the tethers correlates well with the measured *Q*. This work is the first to demonstrate one-dimensional PnC tethers for electrostatic bulk acoustic resonators.

INTRODUCTION

The search for a clear and well-defined relationship between elastic energy dissipation and the quality factor (*Q*) of a mechanical resonator is complicated by the number of dissipation mechanisms that exist in any real vibrating microelectromechanical system (MEMS). These dissipation mechanisms can be categorized as intrinsic mechanisms, such as phonon [1], electron [2], and thermoelastic damping [3], and extrinsic mechanisms, such as viscous damping [4], interface loss, and tether loss [5]. The situation is further compounded by the fact that there has been very limited success in acquiring direct, independent measurements of individual mechanisms of energy loss. Instead, most studies rely on analytical relationships, computational models, and empirical fitting to approximate the underlying physics.

Here, we focus on one of the design-dependent extrinsic energy loss mechanisms: tether loss. Tether loss (also known as anchor, clamping, or acoustic radiation loss) is the result of strain energy transmitted from the driven resonator through the supporting tethers and lost to the anchoring substrate. There have been efforts to model this loss analytically for some canonical geometries [6], to use computational methods to predict the loss [5, 7], and to reconcile these models with experimental data. There have also been efforts to reduce tether loss by designing efficient tethers (quarter-wave tethers, one-dimensional (1-D) or 2-D phononic crystal (PnC) tethers [8, 9]) or by modifying the resonator itself to better confine strain energy away from the tethers [10]. These efforts have relied on theoretical models and measurements of aggregate resonator *Q* without measuring the actual energy flux through the tether.

This paper provides the first direct measurements of the strain energy dissipation profiles along the tethers of mechanical microresonators and clearly demonstrates the difference between efficient and inefficient designs. We use an optical reflection technique that relies on photoelastic modulation of reflected light due to the harmonic strain in the resonator [11] to measure the spatially resolved strain profile on the resonator surface and along the tether. We compare data for a set of conventional and 1-D PnC tether designs for identical silicon bulk acoustic resonators (SiBARs) and verify that the energy lost through the PnC tethers is lower and well correlated with higher resonator *Q*.

EXPERIMENTAL DETAILS

Resonator and Tether Design

Tether loss affects all mechanically supported vibrating devices. The photoelastic measurement used in this work to characterize tethers can be broadly applied to a variety of materials, designs, and frequency ranges. We have selected width-extensional mode SiBARs because they have a well-known electrostatic actuation model, simple design, repeatable fabrication, well-known material properties, and crucially, the ability to make monolithic, single material, low-loss resonators with no material interfaces losses. The SiBARs presented in this work were all fabricated on the same wafer, and have the same nominal dimensions (80 µm × 25.5 µm × 10 µm, $L \times w \times t$), with an actuation gap of ≈ 500 nm on each side. The width is the primary frequency determining dimension. Each SiBAR has a different design for its symmetric tethers. We use four conventional tether designs with lengths equal to $\lambda/8$, $\lambda/4$, $3\lambda/8$, and $\lambda/2$, where $\lambda = w \times 2$ is the acoustic wavelength (Fig.1a).

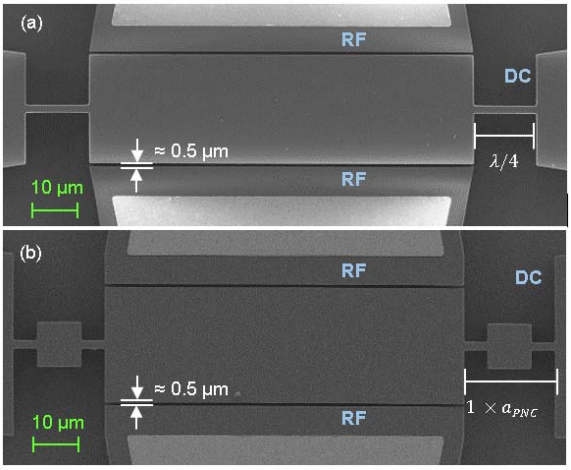

Figure 1: Scanning electron microscope (SEM) image of identical SiBARs (80 µm×25.5 µm×10 µm) with (a) straight tethers of length λ/4, and (b) 1-period PnC tethers.

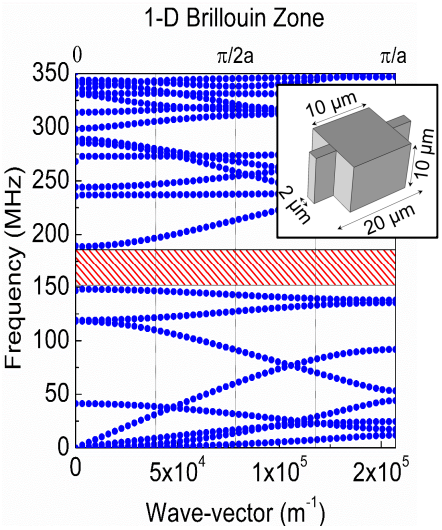

Figure 2: The 1st Brillouin zone for a 1-D phononic crystal unit cell (dimensions in the inset schematic). This PnC design has a wide phononic bandgap (in red) in the frequency range 149 MHz to 188 MHz. a = unit cell length

We also designed a 1-D tether comprised of repeated PnC unit cells (Fig. 1b) with an ideal phononic bandgap between 149 MHz to 188 MHz (Fig. 2), easily blocking the SiBAR fundamental resonance frequency, which is expected to be ≈ 164 MHz from analytical calculations. To test the dependence of the bandgap on the number of unit cells in a real resonator, PnC tethers with 1, 3 and 5 unit cells are used.

Fabrication Process

Standard MEMS fabrication processes are used to make the SiBARs [11]. The process starts with a silicon-on-insulator (SOI) wafer (10 μm device layer, 2 μm buried oxide layer). Metal electrodes are patterned using lift-off and electron-beam evaporation. The resonator, tethers, and actuation gap are defined using optical lithography and etched using deep reactive ion etching (DRIE). The resonators are released by etching the buried oxide using vapor hydrofluoric acid. The structure of the resonator and tethers is fully monolithic and made only of single crystal silicon.

Measurement Principle & Experimental Setup

Driving the resonator into harmonic motion using DC + RF electrostatic actuation causes a harmonic change in the strain at every point on the resonator surface. This periodic strain modulates the refractive index of the material due to the photoelastic effect, and thus modulates the reflection amplitude of a normally incident probe laser. A simplified schematic of the experimental set-up is shown in Fig. 3. An intensity-stabilized He-Ne laser is collimated and focused onto the device with a 20X microscope objective (NA = 0.42, spot size ≈ 2 μm). The reflected signal, measured by a photodetector and network analyzer, provides information about the mechanical motion, including the Q. The amplitude variation as the laser is scanned along the resonator surface enables reconstruction of the strain profile in the plane [11].

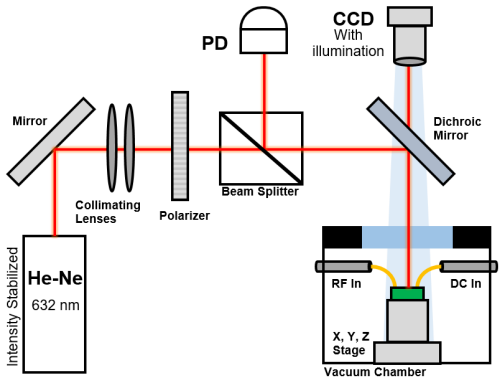

Figure 3: A simplified schematic depicting the measurement setup for photoelastic modulation measurements of in-plane dynamic strain in MEMS resonators, tethers and anchors.

This technique can be used to measure the strain profile along the tethers and on the anchors/substrate. As the tethers are not being actively driven into motion, we expect that the strain decays as we move further from the driven resonator. The spatial rate of decay of the mechanical strain along the length of the tethers is a measure of the tether loss, independent of the other dissipation mechanisms in the environment or the body of the resonator itself. It is expected that an efficient tether design has a high decay rate, and does not allow significant transmission of strain energy to the anchors. Thus, this new technique can directly compare resonator tethers and determine the most efficient designs.

EXPERIMENTAL RESULTS

Spectral Response

The SiBARs are actuated electrically (+21 V DC, +10 dBm RF). The average resonance frequency was 167.041 MHz (σ = 0.039 %). The spectral response of three representative devices is shown in Fig.4, showing the influence of the tether design on the performance of otherwise identical resonators.

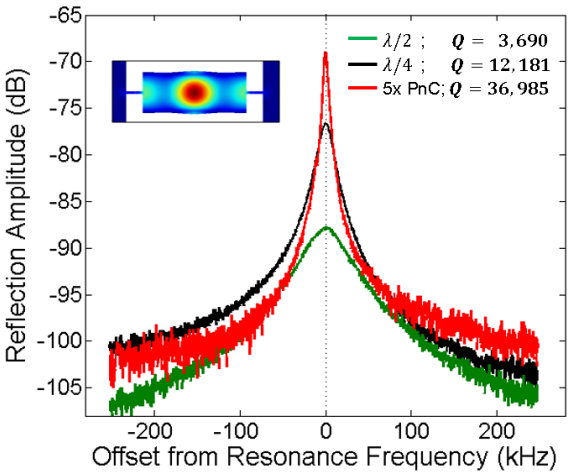

Figure 4: Photoelastic reflection response for three identical SiBARs with different tether configurations. The PnC tethers result in a significantly sharper and stronger mechanical resonance. Inset: Vibrational mode shape of the SiBAR at resonance, showing in-plane strain.

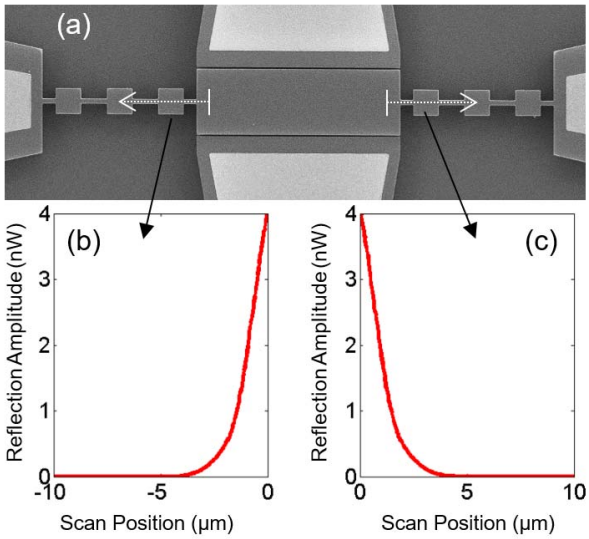

Figure 5: (a) SEM image of a 3-period SiBAR showing the scan vectors for both tethers, with measured reflection amplitude profiles for the (b) left and (c) right tethers.

Tether Profiles

The SIBAR was scanned relative to the probe laser along the length of the tethers using a positioner stage. The spatial rate of decay of the reflection signal along both tethers of each SiBAR was measured, with at least two data sets per tether. To minimize any effect of positioning error, scans were started 5 μm before the root of the tether (on the body of the resonator) and moved towards the anchors. Scans were automated and the positioner stage moved in steps of ≈ 30 nm. Feedback control was implemented to maintain the root mean square (RMS) position error of the stage to under ± 2 nm per step. The reflection amplitudes measured at the network analyzer are proportional to the actual strain. Fig. 5 shows a 3-period PnC tether SiBAR with the scan directions indicated, and the measured profiles along both tethers.

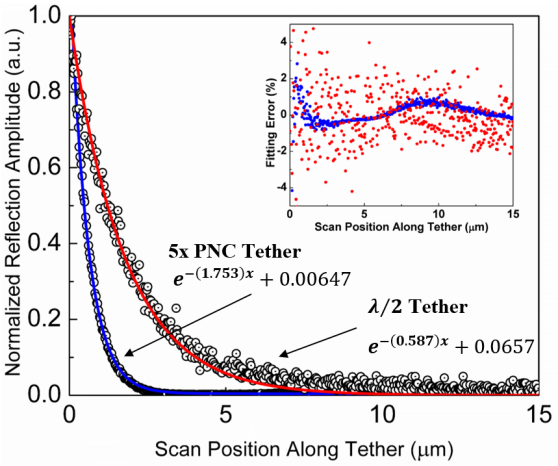

Figure 6: Tether profiles (normalized to full span of each data set) and best-fit exponential curves of the form $(y/y_0 = e^{-\beta x} + c)$ *for two extreme tether designs: a λ/2 beam tether and a 5-period PnC tether. Values of β are in* μm^{-1}*. Inset: The fitting error is less than 5% over the entire range.*

Each dataset has been fitted to an exponential curve of the form $y/y_0 = e^{-\beta x} + c$, using a robust least squares algorithm, where β (μm^{-1}) is the spatial rate of decay. The fitting algorithm searches for the minimum residual fitting error and optimizes starting position and size of a sliding data window to eliminate potential positioning offset errors. Fig. 6 shows two extreme tether strain profiles and best-fit exponential curves. For the purposes of comparison, each data set is normalized to span the full scale between the maximum value at the root of the tether and the minimum value at the system noise floor. The comparison clearly shows the sharp decay for the 5-period PnC tether (Q = 36,985) in contrast to the slow decay for the λ/2 beam tether (Q = 3,690).

TETHER LOSS AND QUALITY FACTOR

The measured values of mechanical Q and the best-fit values of β are plotted in Fig. 7 as a function of the tether design (length or number of periods). For the conventional straight tethers, the relation between length of the tether and the acoustic wavelength is critical, with the λ/4 tether significantly outperforming the λ/2 tether. This experimentally verifies established results based on transmission theory for acoustic/electromagnetic waves. At the same time, we see that the 1-D PnC tethers outperform even the λ/4 tethers significantly, yielding higher Q and sharper damping curves.

For an infinite chain of PnC units, one should see perfect isolation, and an abrupt drop in strain levels at the root of the tether. In a finite PnC chain, we expect sharp, but not abrupt changes in strain levels. As the number of unit cells is increased (which better approximates an infinite phononic crystal), we should expect better performance from the tether. Some evidence of this effect has been demonstrated in the past [8, 12]. Only a slight improvement is found in the present data for PnC tethered SiBARs. This is potentially due to the fact that the PnC tethered SiBARs measured here are limited by intrinsic phonon damping in the Akhieser regime [1], and any increase in Q due to better tether design would be suppressed by phonon damping (Fig. 8).

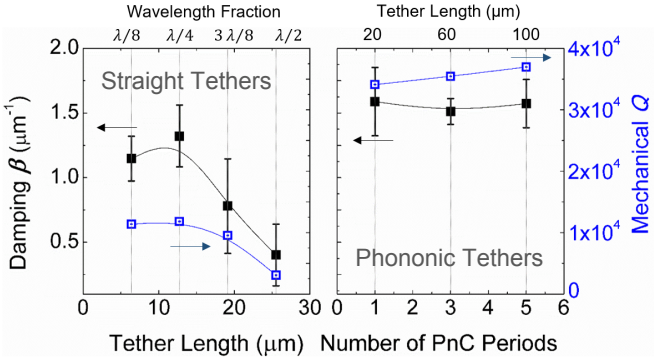

Figure 7: Measured Q (blue open squares) and best-fit β (black closed squares) of straight and PnC tethers. Values of β are averages of 4 data-sets each (two per tether); error bars show one standard deviation. PnC tethers show consistently better Q (lowest Q value for PnC tethers is 2.9 times better than the highest Q value for straight tethers).

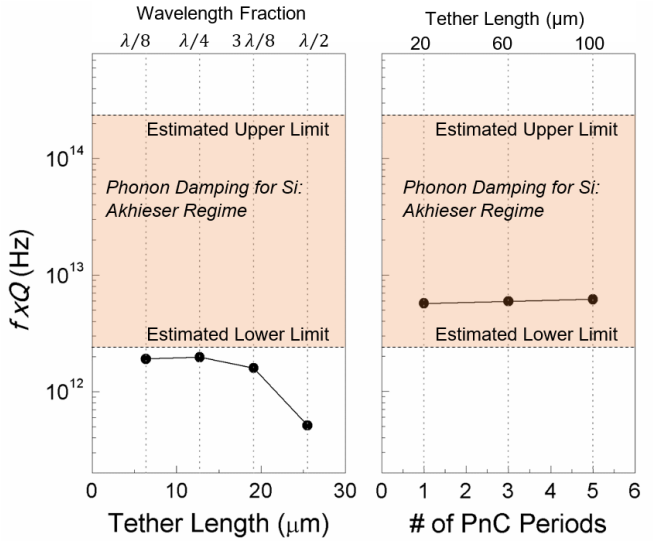

Figure 8: Measured f×Q values indicate that for the same resonator design and fabrication, phononic tethers outperform conventional beam tethers. Further, the PnC tethered resonators are potentially only limited by Akhieser loss. Akhieser damping limit estimates derived from [1].

CONCLUSION

We have demonstrated the first implementation of 1-D PnC tethers for single-material SiBARs. Significant improvement in the mechanical *Q* has been systematically demonstrated using PnC tethers as compared to even the best straight beam tethers. The results indicate that the SiBARs are limited by tether loss or phonon loss; by eliminating tether loss using PnC tethers, the resonators appear to be phonon scattering limited. These SiBARs can be used as high-quality test platforms for gaining a better experimental understanding of phonon loss in silicon, as well as other materials, and be implemented over a wide frequency range.

The scanning strain measurement technique presented here enables spatially resolved visualization of the in-plane dynamics of MEMS resonators and their supporting tethers and anchors in ways that aggregate measurements of electrical parameters cannot accomplish. It provides the ability to measure tether loss profiles directly and independently, and correlate the behavior of various tether designs with the mechanical *Q* of the resonator. Future research shall aim to achieve quantitative, calibrated strain measurements and an analytical relation between the decay rate and *Q*. The ability to separate and evaluate tether loss experimentally, especially for in-plane strain, has broader implications for design optimization and verification of a wide range of mechanically suspended devices including resonators, accelerometers, and gyroscopes.

ACKNOWLEDGEMENTS

This work was supported by DoC/NIST Award # 70NANB14H253 and performed in part in the NIST Center for Nanoscale Science and Technology Nanofab.

REFERENCES

[1] S. Ghaffari, S. A. Chandorkar, S. Wang, E. J. Ng, C. H. Ahn, H. Vu, *et al.*, "Quantum Limit of Quality Factor in Silicon Micro and Nano Mechanical Resonators," *Scientific Reports,* vol. 3, p. 3244, 2013.

[2] V. J. Gokhale and M. Rais-Zadeh, "Phonon-electron interactions in piezoelectric semiconductor bulk acoustic wave resonators," *Scientific Reports,* vol. 4, p. 5617, 2014.

[3] A. Duwel, R. N. Candler, T. W. Kenny, and M. Varghese, "Engineering MEMS Resonators With Low Thermoelastic Damping," *IEEE/ASME Journal of Microelectromechanical Systems* vol. 15, pp. 1437-1445, 2006.

[4] M. Bao and H. Yang, "Squeeze film air damping in MEMS," *Sensors and Actuators A: Physical,* vol. 136, pp. 3-27, 2007.

[5] A. Frangi, M. Cremonesi, A. Jaakkola, and T. Pensala, "Analysis of anchor and interface losses in piezoelectric MEMS resonators," *Sensors and Actuators A: Physical,* vol. 190, pp. 127-135, 2013.

[6] Z. L. Hao, A. Erbil, and F. Ayazi, "An analytical model for support loss in micromachined beam resonators with in-plane flexural vibrations," *Sensors and Actuators A-Physical,* vol. 109, pp. 156-164, 2003.

[7] D. S. Bindel and S. Govindjee, "Elastic PMLs for resonator anchor loss simulation," *International Journal for Numerical Methods in Engineering,* vol. 64, pp. 789-818, 2005.

[8] H. Zhu and J. E. Y. Lee, "Design of Phononic Crystal Tethers for Frequency-selective Quality Factor Enhancement in AlN Piezoelectric-on-silicon Resonators," *Procedia Engineering,* vol. 120, pp. 516-519, 2015.

[9] L. Sorenson, J. L. Fu, and F. Ayazi, "One-dimensional linear acoustic bandgap structures for performance enhancement of AlN-on-Silicon micromechanical resonators," in *16th International Solid-State Sensors, Actuators and Microsystems Conference (Transducers '11)*, 2011, pp. 918-921.

[10] J. Zou, C.-M. Lin, and A. P. Pisano, "Quality factor enhancement in Lamb wave resonators utilizing butterfly-shaped AlN plates," in *IEEE International Ultrasonics Symposium*, 2014, pp. 81-84.

[11] V. J. Gokhale and J. J. Gorman, "Dynamic characterization of in-plane bulk acoustic resonators using high-sensitivity optical reflection measurements," in *Solid-State Sensors, Actuators, and Microsystems Workshop*, Hilton Head Island, 2016, pp. 145-148.

[12] D. Feng, D. Xu, G. Wu, B. Xiong, and Y. Wang, "Phononic crystal strip based anchors for reducing anchor loss of micromechanical resonators," *Journal of Applied Physics,* vol. 115, p. 024503, 2014.

CONTACT

*Jason J. Gorman, email: gorman@nist.gov